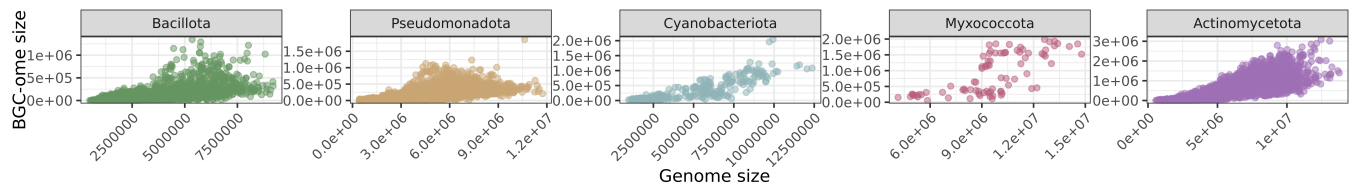
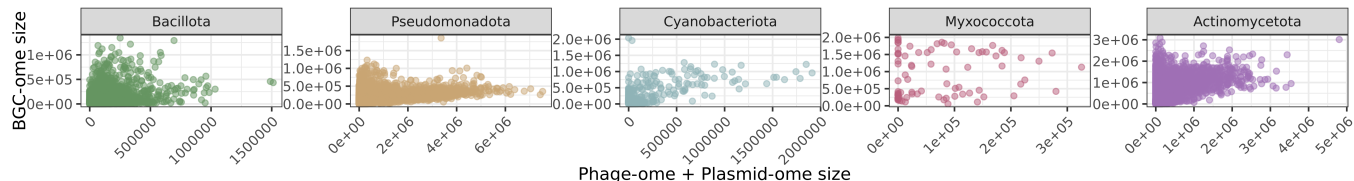
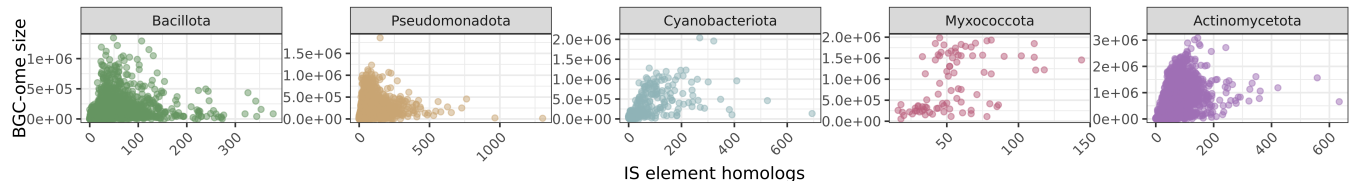
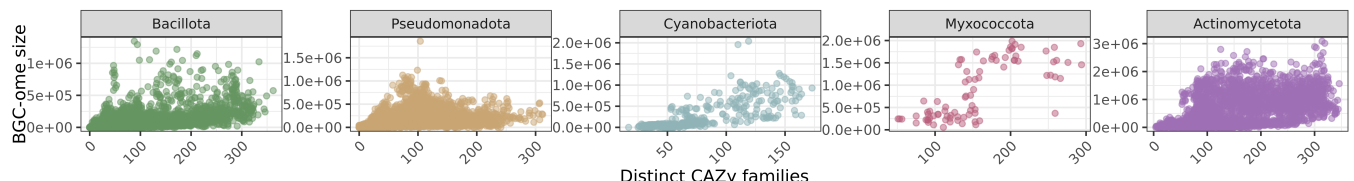
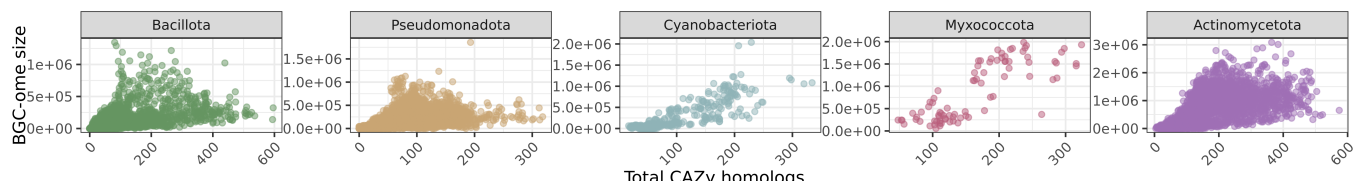
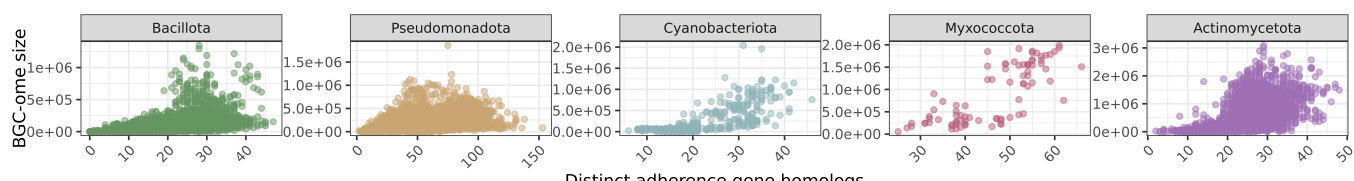
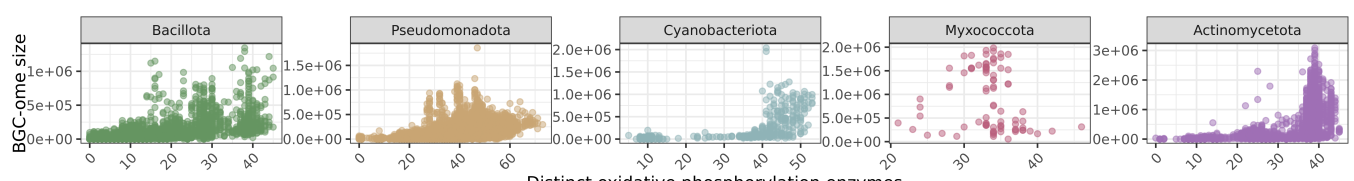
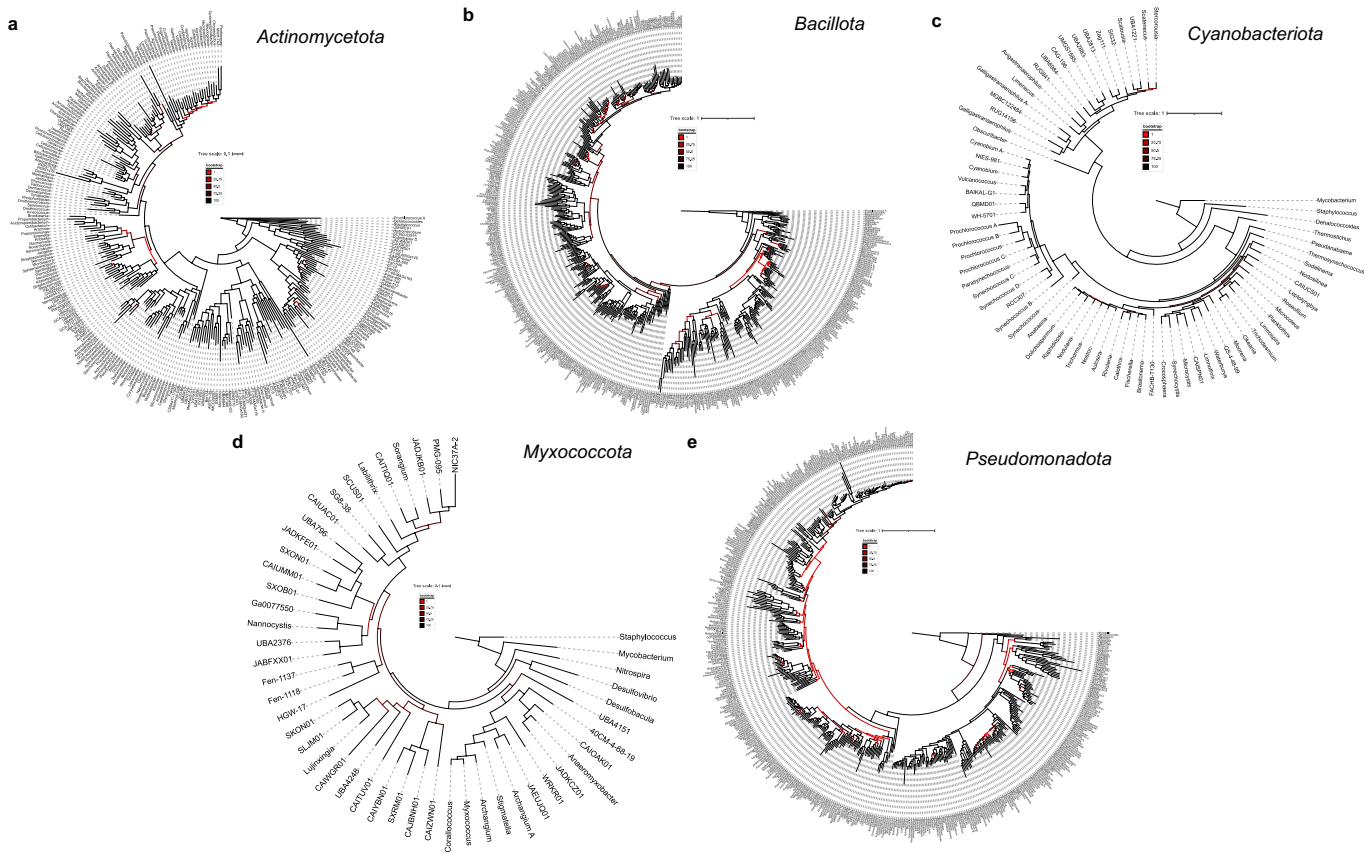
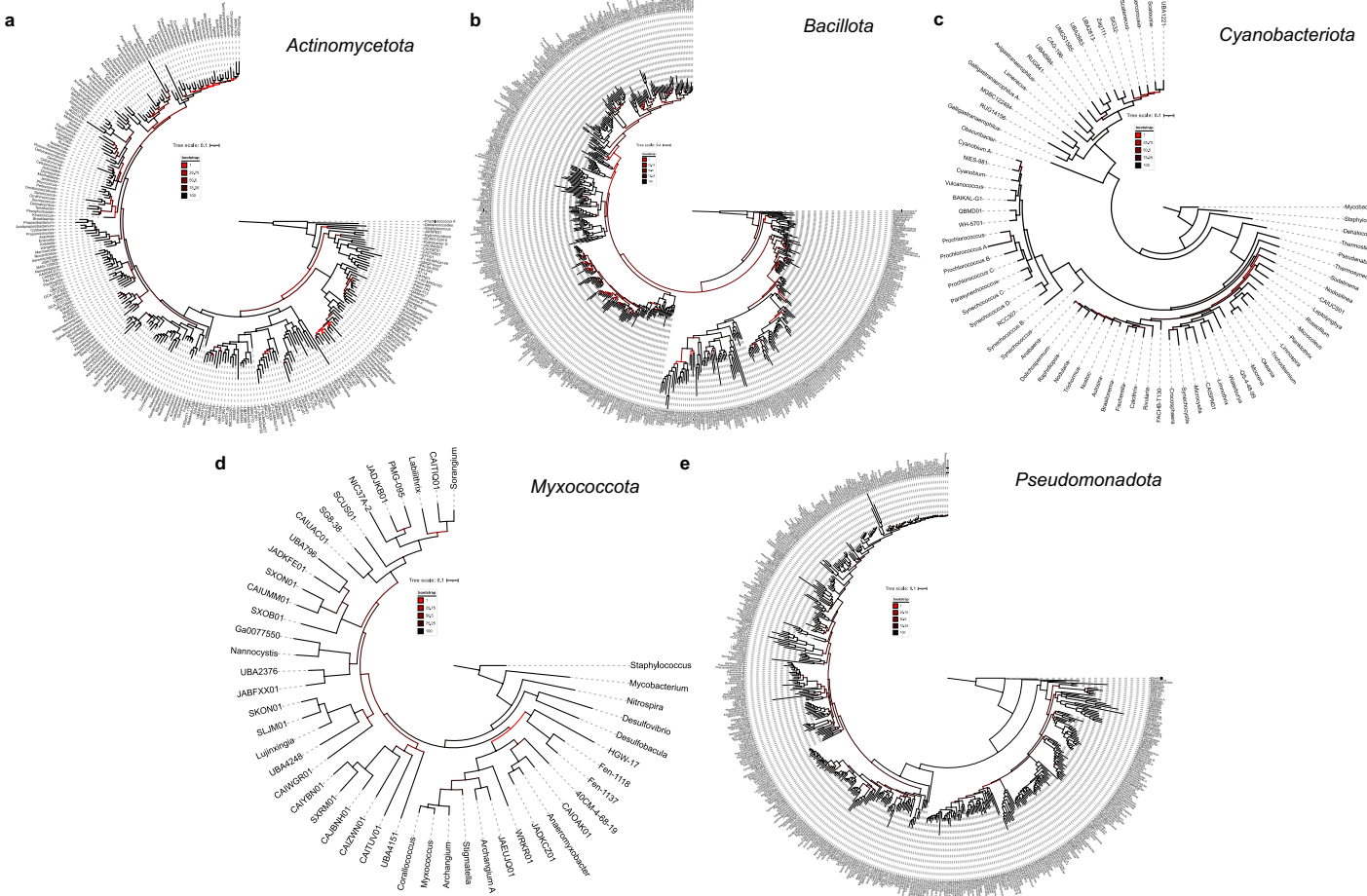


a**b****c****d****e****f****g**

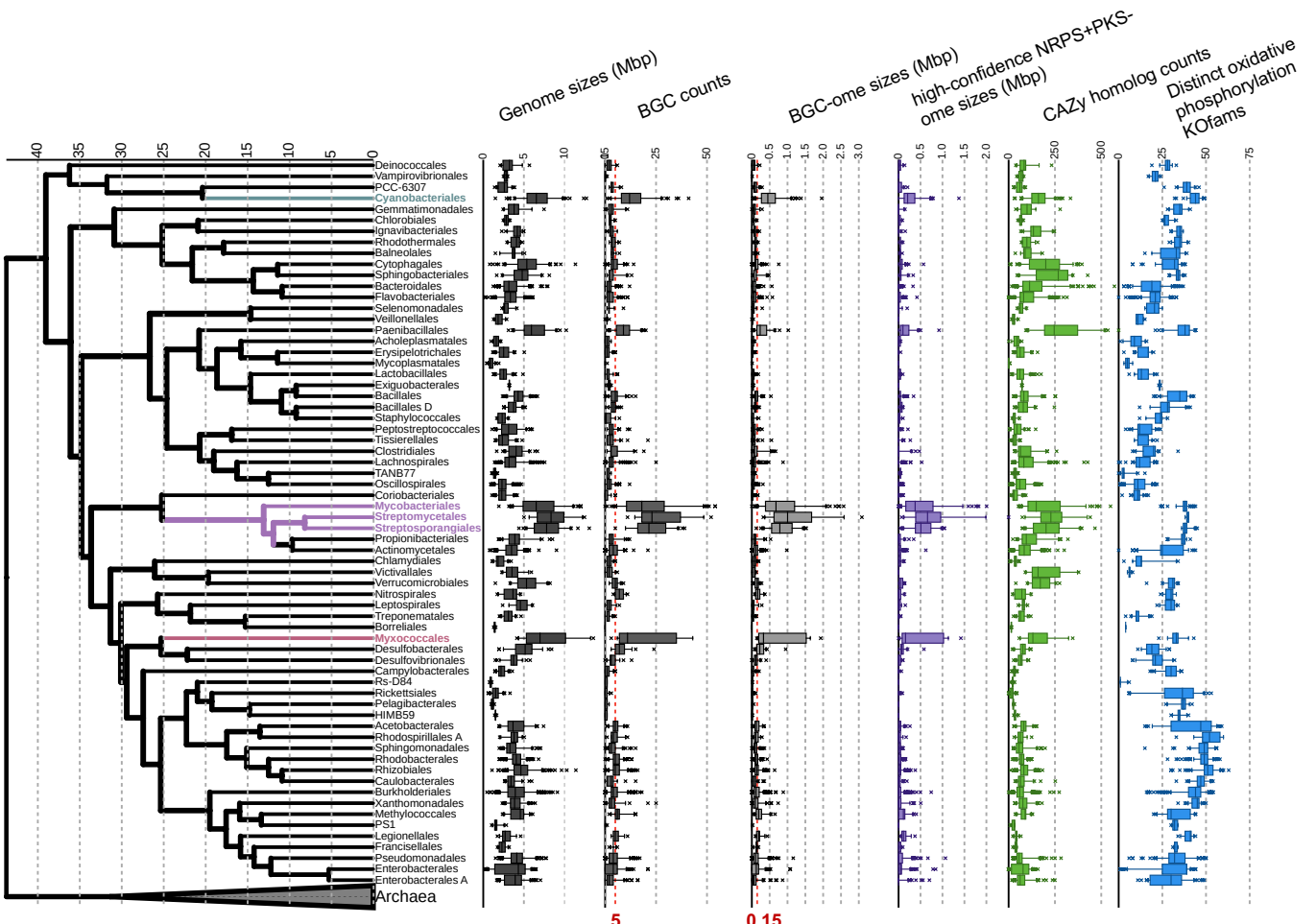
Sup Fig. A | Relationships between genetic factors and BGC-ome size in five bacterial phyla. Scatterplots depicting the relationship between the BGC-ome size and **a**, genome size, **b**, predicted phage-ome + plasmid-ome size, **c**, transposon homolog count, **d**, distinct CAZy families count, **e**, total CAZy homolog count, **f**, adherence gene homolog count, **g**, distinct oxidative phosphorylation enzyme counts.



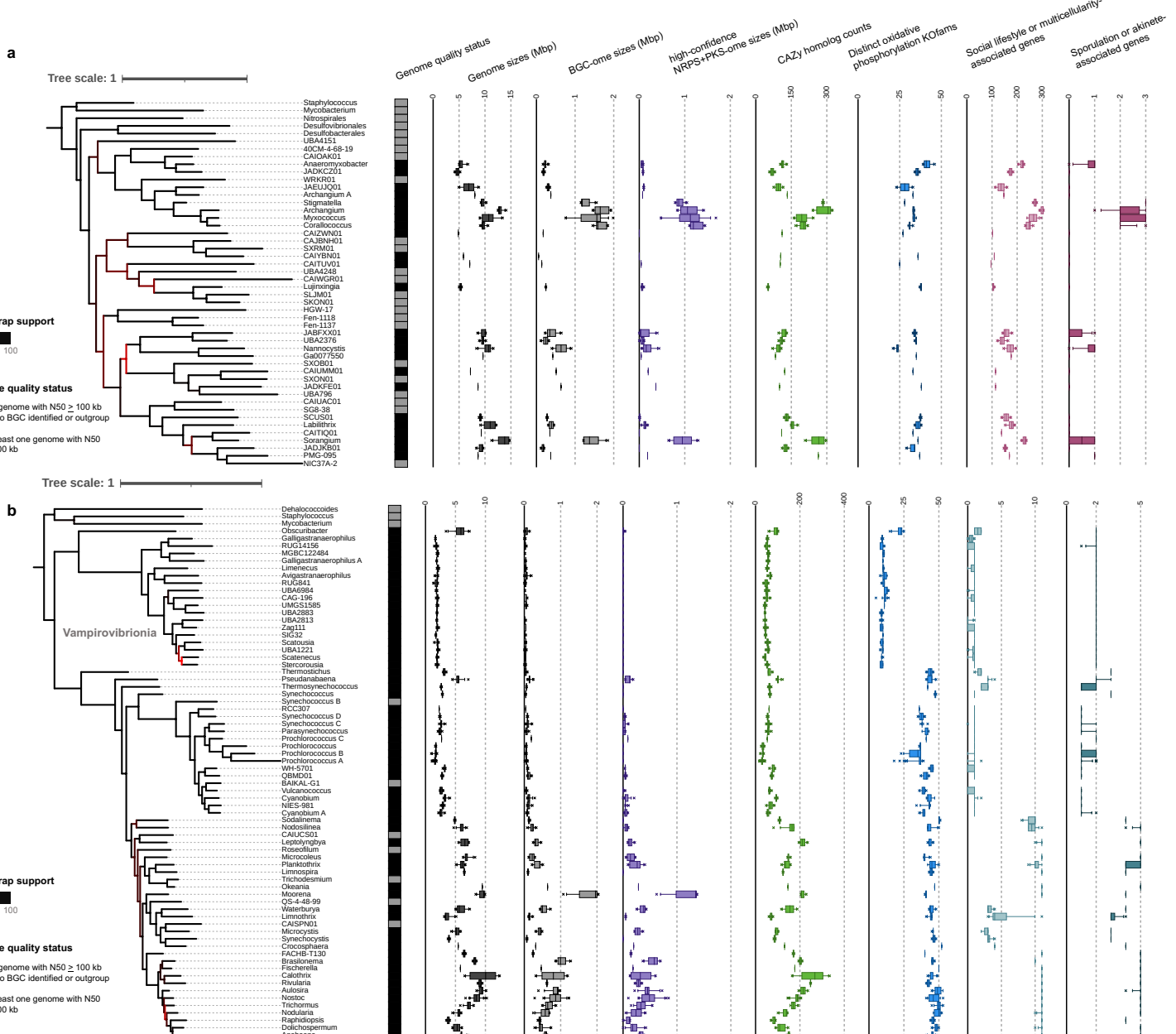
Sup Fig. B | Phylogenomics of five bacterial phyla with information on biosynthetic capabilities (without removal of high heterogeneity sites). Maximum-likelihood phylogenies using IQ-Tree on largely, single-copy-core ortholog group alignments for **a**, Actinomycetota, **b**, Bacillota, **c**, Cyanobacteriota, **d**, Myxococcota and **e**, Pseudomonadota are shown.



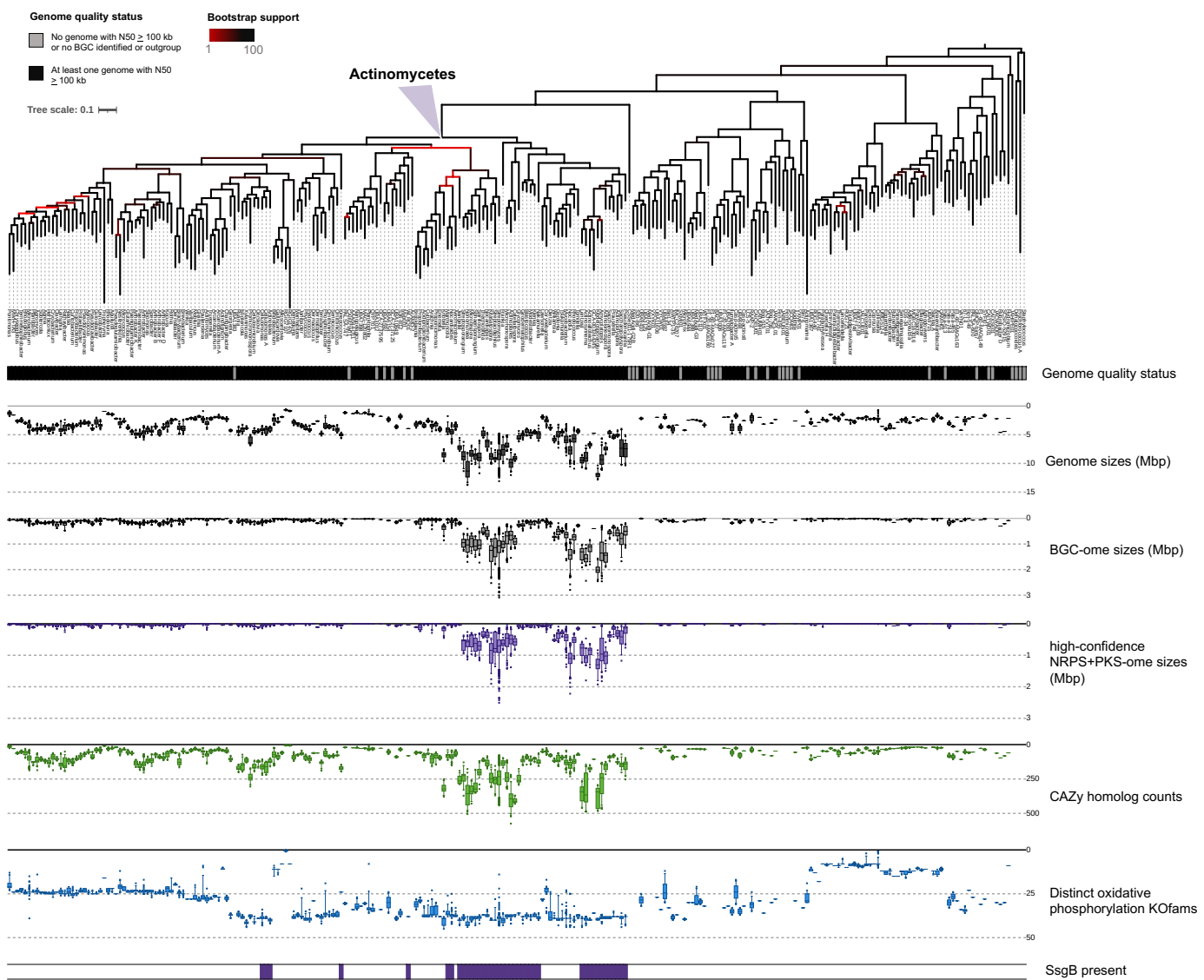
Sup Fig. C | Phylogenomics of five bacterial phyla with information on biosynthetic capabilities (with removal of high heterogeneity sites). Maximum-likelihood phylogenies using IQ-Tree on largely, single-copy-core ortholog group alignments after removal of high heterogeneity sites for **a**, *Actinomycetota*, **b**, *Bacillota*, **c**, *Cyanobacteriota*, **d**, *Mixococcota* and **e**, *Pseudomonadota* are shown. Branch coloring indicates bootstrap support.



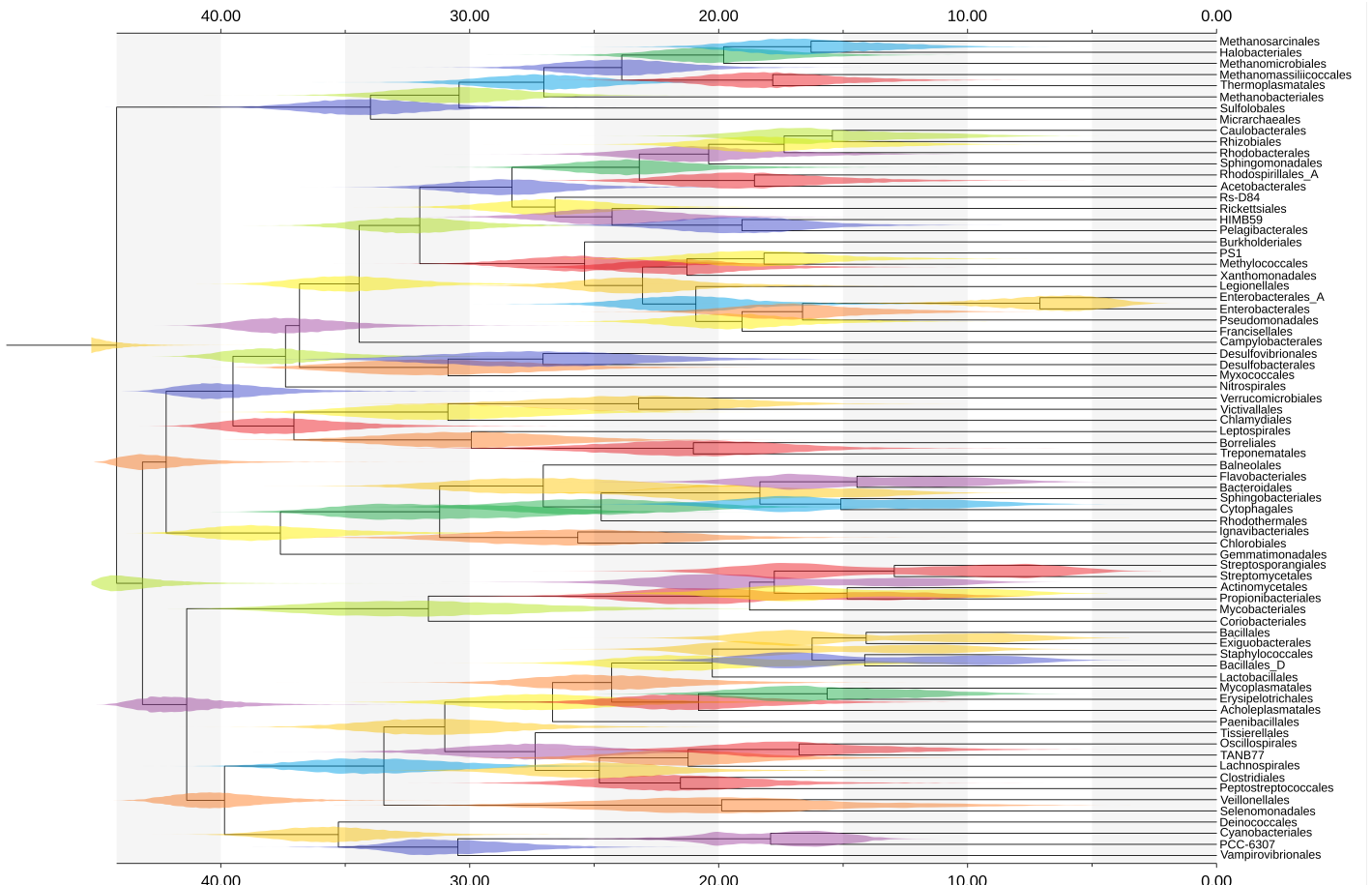
Sup Fig. D | Genome, BGC-ome sizes, and CAZy homolog counts across the bacterial tree of life. Distributions for genome sizes (dark grey), BGC counts (grey), BGC-ome sizes in Mbp (light-grey), high-confidence NRPS & PKS BGC sums (purple), total number of CAZy homologs (green), and the number of distinct oxidative phosphorylation KOfams (blue) are shown for representative orders across the bacterial tree of life.



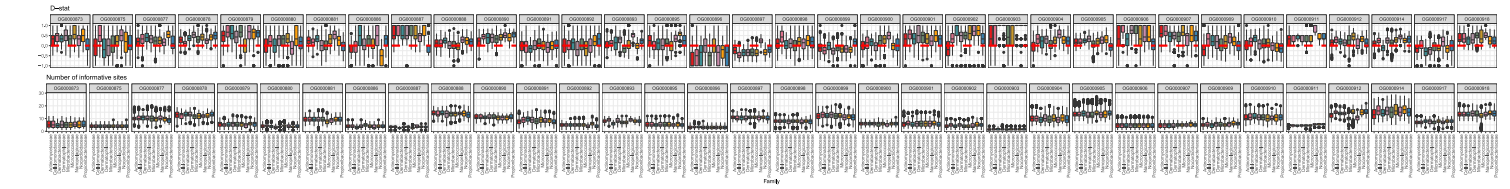
Sup Fig. E | Phylogenetic views of BGC-ome size, multicellularity-associated gene counts, and sporulation-associated gene counts for Cyanobacteriota and Myxococcota. Distributions for genome sizes (dark grey), BGC-ome sizes (grey), high-confidence NRPS & PKS BGC sums (purple), total CAZY homologs (green), oxidative phosphorylation enzymes (blue), multicellularity or social-lifestyle associated genes (light violet and light teal), and sporulation or akinete associated genes (dark violet and dark teal) are shown for representative genera from **a**, Myxococcota and **b**, Cyanobacteriota.



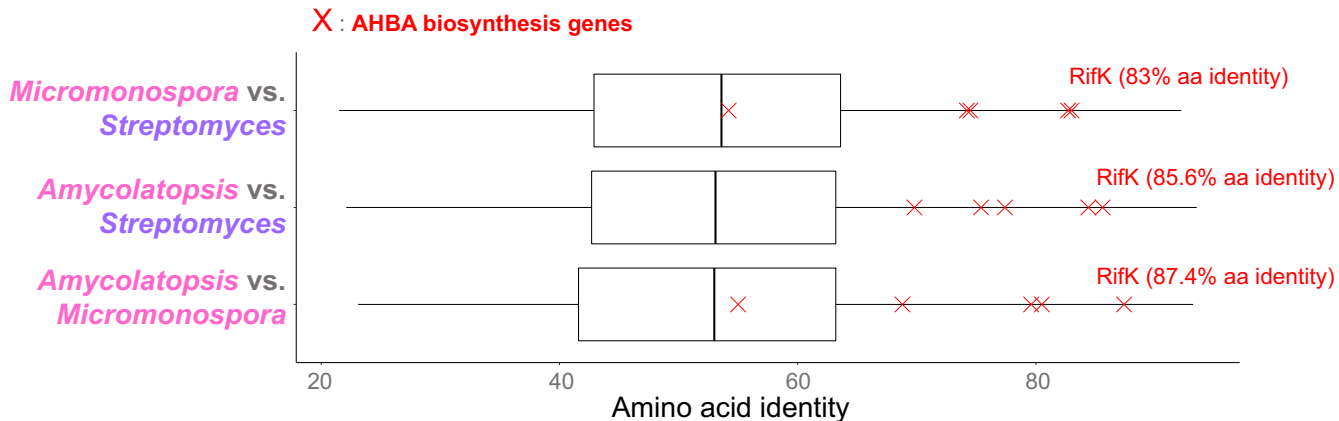
Sup Fig. F | Phylogenetic view of BGC-ome size, multicellularity-associated gene counts and sporulation-associated gene counts for *Actinomycetota*. Distributions for genome sizes (dark grey), BGC-ome sizes (grey), high-confidence NRPS & PKS BGC sums (purple), total CAZy homologs (green), oxidative phosphorylation enzymes (blue), and the presence of the sporulation/multicellularity-associated marker SsgB (dark purple) are shown for representative genera from *Actinomycetota*.



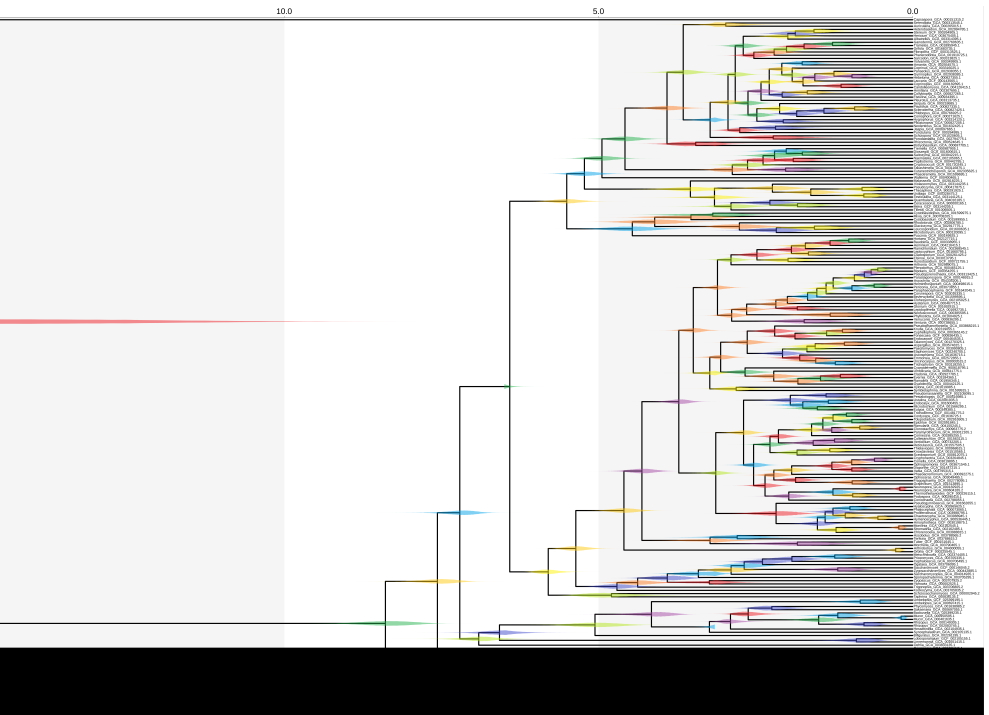
Sup Fig. G | Timetree of bacterial and archaeal orders. MCMCTree was used to perform divergence dating between bacterial and archaeal order representative genomes. The initial phylogeny was created using IQ-TREE with a heterotaxy aware model and significant topological constraints imposed based on higher-resolution phylum specific topologies and literature. Visualization was performed using TreeViewer with posterior age distributions shown for each innernode.



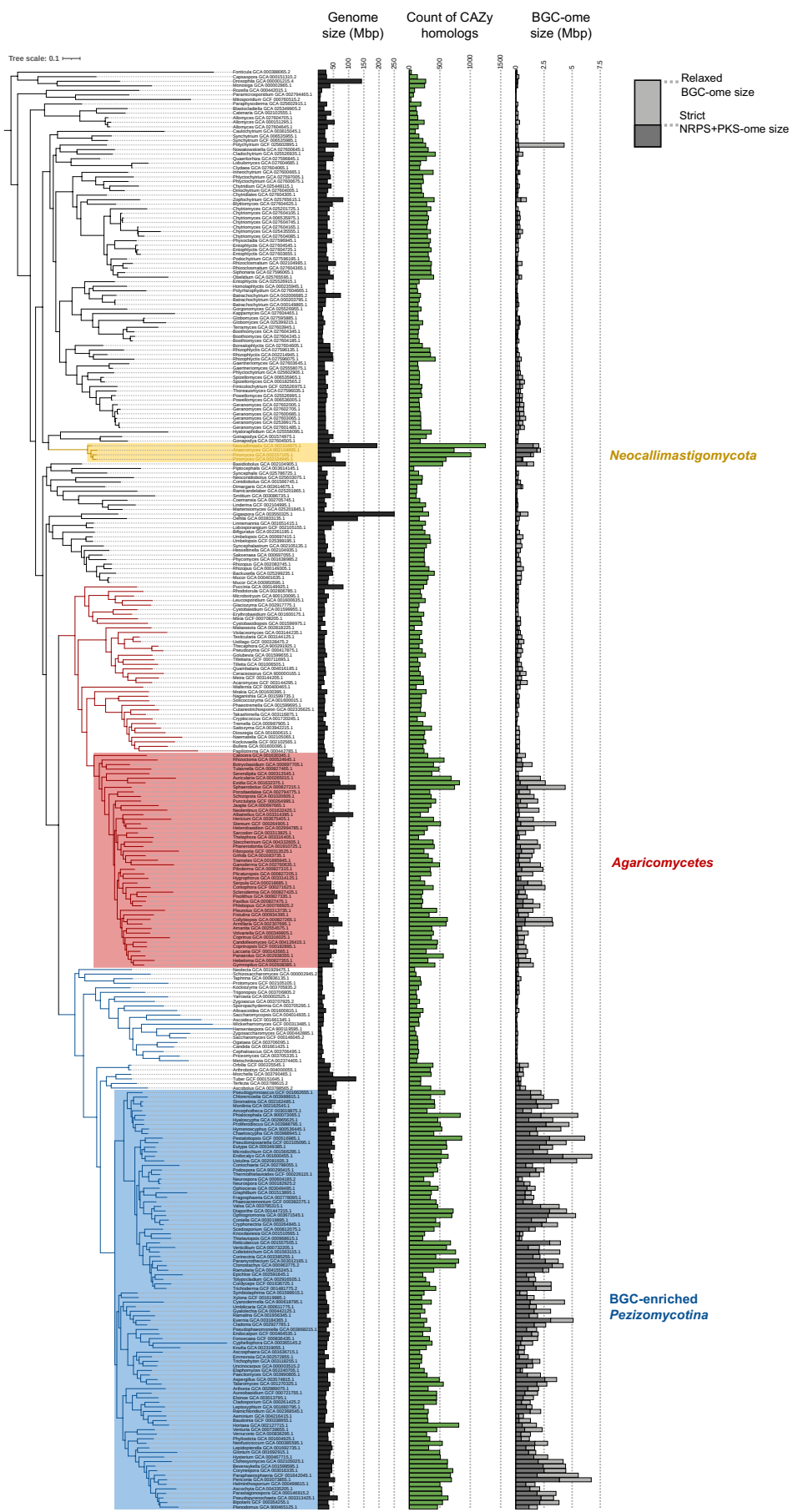
Sup Fig. H | D.stat calculations per single-copy core ortholog group. The distribution of the D.stat is shown for each single-copy-core ortholog group independently (top row), together with the number of informative sites assessed (bottom row).



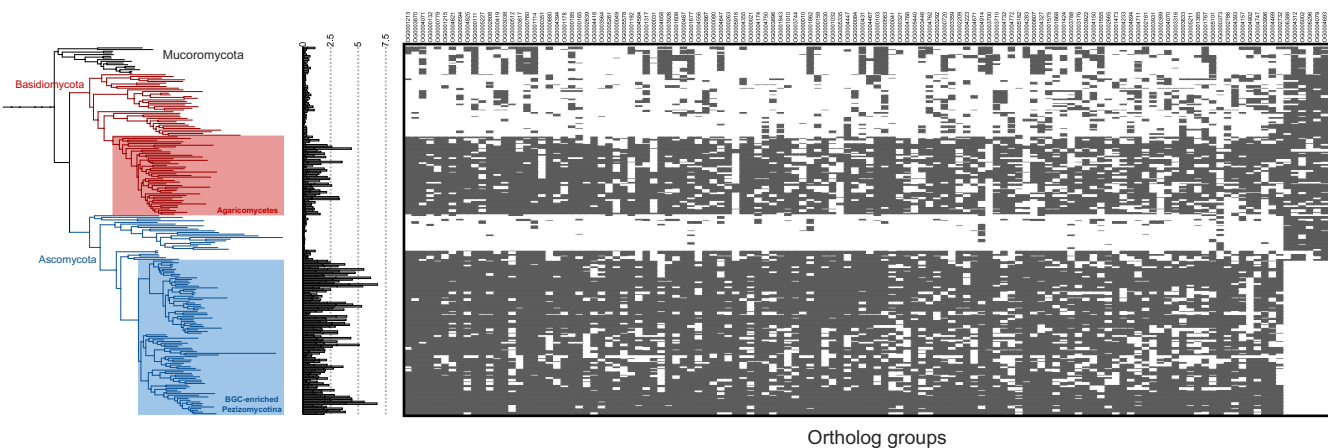
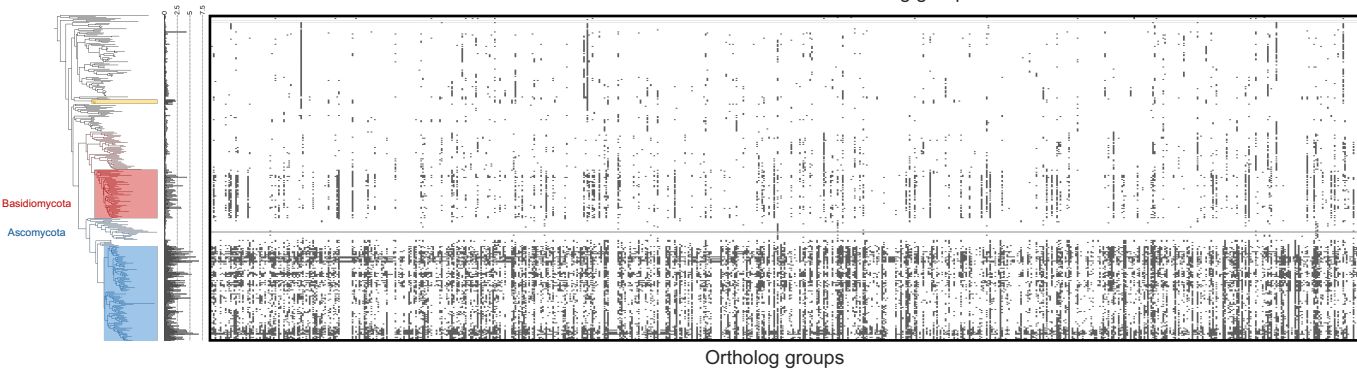
Sup Fig. I | Pairwise amino acid identity distributions of orthologs between genomes with rifamycin and chaxamycin BGCs. The amino acids between orthologs identified by OrthoFinder analysis were systematically computed using paiof between three genomes deemed to carry rifamycin (*Amycolatopsis* & *Micromonospora*) or chaxamycin (*Streptomyces*) BGCs. The identity of orthologs corresponding to AHBA biosynthesis genes are noted as red crosses. Boxplot is in Tukey's style.



Sup Fig. J | Timetree of select fungal representatives. MCMCTree was used to perform divergence dating between 212 representative fungal genomes, including an outgroup (*Capsaspora*) used for rooting. The initial phylogeny was created using IQ-TREE with a heterotachy aware model. Visualization was performed using TreeViewer with posterior age distributions shown for each innernode. The age scale is in 100 Mya.



Sup Fig. K | Detailed view of fungal phylogeny. A rectangular version of the fungal phylogeny from Fig. 3a is shown featuring leaf labels as well.

a**b**

Sup Fig. L | Phylogenetic distribution of ortholog groups significantly associated with BGC-ome size and differentially found between Agaricomycetes & BGC-enriched Pezizomycotina in comparison to other Dikarya. **a.**, The distribution of 672 ortholog groups identified by GWAS analysis as significantly associated with BGC-ome size are shown. Ortholog groups are arranged in increasing order by the phylogeny-corrected p -value for the association. **b.**, The distribution of 124 ortholog groups identified by comparative genomics as differentiating between the BGC-rich clades of BGC-enriched Pezizomycotina and Agaricomycetes and other Dikaryon species is shown across the subkingdom of Dikaryon and neighboring phylum of Mucromycota. Ortholog groups are arranged in decreasing order by the difference in conservation between the two groups.